Modeling of multi-wavelength Raman fiber lasers using a new and fast algorithm

Florence Leplingard, Catherine Martinelli, Sophie Borne, Laurence Lorcy, Thierry Lopez, Dominique Bayart, François Castella, Philippe Chartier, and Erwan Faou

***Abstract*— We describe the numerical model of a multi-wavelength Raman fiber laser. It uses an original algorithm which makes the model robust and fast. Comparison between simulation and experiment on Raman laser output power, characterized by the slope efficiency and the threshold, are presented.**

***Index Terms*—Modeling, numerical analysis, optical fiber lasers, Raman lasers.**

I. Introduction

Distributed Raman amplification is a key technology to reduce the cost of long-haul WDM transmission systems. Indeed, it allows to lower the effective noise figure of the transmission span (allowing to minimize the count of high-cost electrical regenerators used in the network) and offers the possibility to broaden the amplification band. To achieve a broad and flat amplification band, pumping sources with multiple output wavelengths have recently been developed.

An approach is to use Raman fiber lasers. Such a solution is cost-effective because it uses both low-cost fiber components and multi-watt broad area semiconductor lasers. They have also several other advantages: they are not polarized, a single laser can emit simultaneously several output wavelengths (up to 6 have been demonstrated [1]), they are easily scalable in power. Compared to semiconductor modules, the power repartition in the different output wavelengths needs some control due to the interaction between channels in the cavity, but effective and simple operation has been demonstrated [2].

To predict and optimize a multi-wavelength laser, it is required to be able to model such laser. Several papers [3-4] have described numerical models but there are no comparison between the measured and the simulated output powers, especially comparing the simulated and calculated slope efficiencies and pump thresholds. In this paper, we first present our numerical model based on an original, robust and fast algorithm. Then, we describe the characterization of the laser to get the required parameters to introduce in the calculation. Eventually, we present the comparison between experiment and simulation.

Manuscript received April XXX, 2004

F. Leplingard, C.Martinelli, S.Borne, L.Lorcy, T.Lopez., D.Bayart are with Alcatel R&I, route de Nozay, 91461 Marcoussis Cédex, France (phone: 33 1 69 63 47 22; fax: 33 1 69 63 18 65; e-mail: Florence.Leplingard@alcatel.fr).

F.Castella, P.Chartier, E.Faou are with IRISA Rennes, Campus Beaulieu, 35042 Rennes Cédex, France (e-mail: Francois.Castella@univ-rennes1.fr).

II. The numerical model

The algorithm developed for the simulation of the multi-wavelength Raman laser described here is based on the well-known coupled equations described in [3-5]. This model aims at simulating various lasers including multi-wavelength lasers with Stokes close to each other. Since the interactions involved are not only with the closest Stokes, all interactions are considered. The set of equations (1) describes the evolution of the Stokes, where $P_i^+(z)$ and $P_i^-(z)$ are the forward and backward propagating powers for Stokes i at frequency ν_i or wavelength λ_i, z varying between 0 and L, with L length of the Raman fiber:

$$\frac{dP_i^{\pm}}{dz} = \mp\alpha_i P_i^{\pm} \pm \sum_j G_{ij} P_i^{\pm}\left(P_j^+ + P_j^-\right), \quad (1)$$

where:

$$G_{ij} = g_{ij} \qquad if\ i > j$$

$$G_{ij} = -\frac{\lambda_i}{\lambda_j} g_{ij} \qquad if\ i < j$$

$$G_{ii} = g_{ii} = 0$$

α_i is the attenuation of the fiber at λ_i and g_{ij}, the Raman gain coefficient between Stokes i and j.

The description becomes complete upon adding the following boundary conditions:

$$P_1^+(0) = P \text{ and } P_i^+(0) = R_i^0\ P_i^-(0) \quad with\ i = 2\ to\ n, \quad (2)$$

$$P_i^-(L) = R_i^L\ P_i^+(L) \quad with\ i = 1\ to\ n, \quad (3)$$

where P is the launched pump power, R_i^0 and R_i^L are the reflectivities of the mirrors at z = 0 and z = L for Stokes i.

The system (1-3) possesses the `trivial' solution $P_1^+ = P_1^- = P$ and $P_i^+ = P_i^- = 0$ for i>=2. In practice, the laser starts on the noise due to the Amplified Spontaneous Emission (ASE)

which has been neglected in equations (1). From a mathematical point of view, when the ASE term is taken into account, the only admissible regime is the non-trivial one. However, as soon as the laser 'starts', the contribution of the ASE can be completely neglected. The system formed by equations (1), (2) and (3), which is known as a two-point boundary value problem, can be solved using the conventional shooting method. However, using this method, it is necessary to 'guess' the initial conditions (in z = 0 and z = L) and the convergence depends on the good choice of these values. Consequently, if the algorithm does not converge, one can not guarantee that there is no solution to the system. To circumvent this difficulty, a new algorithm has been introduced. It relies on a change of unknowns in equations (1-3), correlated with the existence of invariants in the system. Indeed, from the set of equations (1), one can easily demonstrate that $c_i = P_i^+ . P_i^-$ is a constant. Therefore, equations (1) can be written as:

$$\frac{du_i}{dz} = -\alpha_i + 2\sum_j G_{ij}\sqrt{c_i}\cosh(u_i)$$

$$\frac{dc_i}{dz} = 0$$

where:

$$\frac{du_i}{dz} = \frac{1}{P_i^+}\frac{dP_i^+}{dz}$$

The boundary conditions become:

$$u_1(0) = \log\left(\frac{P}{\sqrt{c_1}}\right) \quad and \quad u_i(0) = \frac{1}{2}\log\left(R_i^0\right) \quad for \quad i = 2 \quad to \quad n$$

$$u_i(L) = -\frac{1}{2}\log\left(R_i^L\right) for \quad i = 1 \quad to \quad n$$

Note that all boundary conditions but $u_1(0)$ are independent of c_i. Therefore, when the coupled equations are written with the new variables, the new equations are defined for any set of initial values. Moreover, the existence and uniqueness of the solution can be proven [6, 7].

As the new algorithm solves the problem encountered without the guess on the initial values, it is therefore faster (less than 1 second) and more robust than the traditional way of solving this type of system. It allows to compute easily, even complicated lasers with several output wavelengths.

III. MEASUREMENTS REQUIRED BY THE MODEL

To simulate a laser, it is necessary to introduce in the model the characteristics of the active and passive components. The structure of a laser is represented in figure 1.

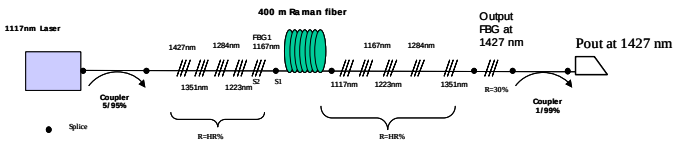

Fig. 1: The structure of a studied Raman fiber laser

The characteristics of the amplifying fiber have to be known. The Raman gain coefficient g_{ij} is a function of the pump Stokes of lower wavelength λ_i and the frequency shift $\Delta\nu = \nu_i - \nu_j$ between Stokes i and j:

$$g_{ij} = g_R(\nu_{ref}, \Delta\nu)\frac{\nu_i}{\nu_{ref}}\frac{A_{eff}(\nu_{ref}, \nu_{ref} - \Delta\nu)}{A_{eff}(\nu_i, \nu_i - \Delta\nu)} \quad , \quad (4)$$

where g_R is the fiber Raman gain coefficient, ν_{ref} is the pump frequency at which the Raman gain coefficient has been measured and A_{eff} (ν_i, ν_j) is the average effective area at frequencies ν_i and ν_j. We have assumed a step index profile with gaussian modes and $A_{eff} = \pi(\omega_i^2 + \omega_j^2)/2$, where ω_k is the waist of the field at ν_k.

The dependence of g_{ij} with the frequency shift $\Delta\nu$, was obtained by measuring the on/off gain of the fiber pumped at 1470 nm with a signal varying over the required frequency shift. The measurement method is described in [8]. The g_{ij} was also measured at a pump wavelength of 1117 nm, using another technique where the ASE is measured. This measurement allowed us to verify that the Raman gain coefficient satisfies (4) between 1117 nm and 1470 nm where the laser is operated. Using (4), we can calculate the Raman gain coefficient at any pump wavelength.

In the model, the lumped loss (splice loss and loss of the Fiber Bragg gratings (FBG)) should be taken into account. To this aim, they are introduced in the reflectivities of the FBG considering that, on a round trip, the field 'sees' twice a lumped loss. Also each lumped loss is taken into account in the embedded cavity within which it lays. For example, the high reflectivity mirror FBG_1 in figure 1, which reflectivity is HR%, has a reflectivity decreased to $HR*10^{(-2S_1/10)}*10^{(-2S_2/10)}$ where S_1 is the lumped loss of the splice and S_2 is the insertion loss of FBG_1 in dB.

Besides, the model does not consider any linewidth for the output spectra of the powers of the Stokes nor for the FBG. In a real laser, several longitudinal modes are able to lase and the linewidth increases with power. Therefore, all the different longitudinal modes of the Stokes in the cavity do not 'see' the same reflectivity. Moreover, if the input and output FBG for a given Stokes is not well centered on the central lasing wavelength, reflectivity of the FBG will decrease. It is possible to introduce an effective reflectivity R_{eff} [9] that can be evaluated by measuring the output power $dP(\lambda_i)$ and the reflectivity $R(\lambda_i)$ of the FBG:

$$R_{eff} = 1 - \frac{\sum dP(\lambda_i)}{\sum \frac{dP(\lambda_i)}{1 - R(\lambda_i)}}, \quad (5)$$

IV. Results and Discussions

Figure 2a represents the simulated results for a Raman laser with an output wavelength of 1427 nm and an output reflectivity of 30%. The structure of the laser is described in figure 1. One can see that the simulation results are very close to those obtained experimentally. There is less than 5% discrepancy between the experimental and the simulated slopes and thresholds. The error on the slope and the threshold is within the measurement accuracy of the reflectivities of the FBG. Other output reflectivities (10%) and other output wavelengths (1455 nm) have been tested for a single output wavelength laser. The simulation results fit the experiment with the same precision.

Raman lasers with two output wavelengths have been simulated and compared to experiment as well. We have simulated a laser with the two output wavelengths on successive gain curves. Such a laser is used for application like second order pumping. Here, the output wavelengths are 1351 nm and 1427 nm. We have also simulated a laser with the two output wavelengths on a same gain curve. The output wavelengths are 1427 nm and 1480 nm. For both lasers, the structure of the laser is similar to figure 1 with the same intermediate Stokes. For the first laser, we have just replaced the output HR FBG at 1351nm by a FBG with a reflectivity of 20%. For the second laser, the FBG at 1427 nm has a reflectivity of 10% and we have added a cavity at 1480 nm, using a 50% FBG for the output. In both cases, the discrepancy on the slope efficiencies is lower than 5% but it is close to 10% on the threshold. As shown on figure 2b, this can be explained by the error on the measurement of the reflectivities of the output FBG (estimated to be 10%).

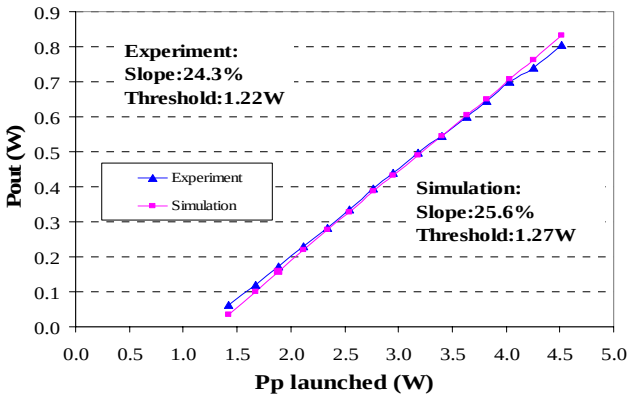

a

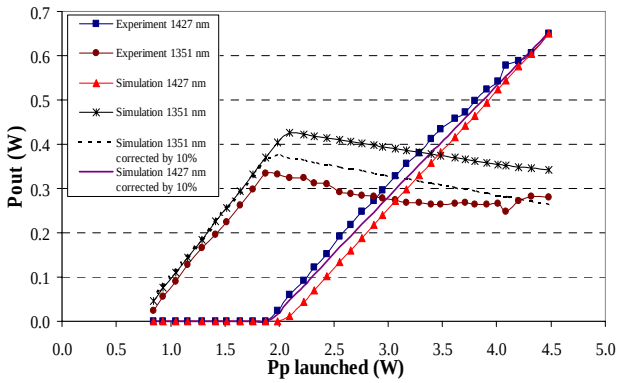

b

Fig. 2: a) Single wavelength laser at 1427 nm b) Dual wavelength laser at 1351 nm and 1427 nm

V. Conclusion

In this paper, we described the model used to simulate a multi-output-wavelength Raman laser. A change of unknowns in the coupled equation system leads to a fast and robust algorithm that ensures the existence and uniqueness of the solution. The fiber characteristics, the lumped loss and the effective reflectivities are measured and introduced in the model. Considering a 10% measurement error on the output reflectivities, the simulated laser thresholds and slopes fit the experiment with a discrepancy lower than 5%. This is the first time, to our knowledge, that such comparisons are done.

References

[1] F. Leplingard, S. Borne, L. Lorcy, T. Lopez, J.J. Guérin, C. Moreau, C. Martinelli, D. Bayart, “Six output wavelength Raman fibre laser for Raman amplification", Electron. Lett., vol. 38, Aug. 2002, pp 886-887

[2] M.D. Melmerstein, C.Horn, Z. Huang, M. Luvalle, J.C. Bouteiller, C. Headley, B.J. Eggleton, “Configurability of a three-wavelength Raman fiber laser for gain ripple minimization and power partitioning", Proc. Optical Fiber Com., March 2002 pp 59-60

[3] M. Rini, I. Christiani, and V.Degiorgio, “Numerical modeling and optimization of Cascaded Raman fiber Lasers”, IEEE Journal of Quantum Electron., vol. 36, Oct. 2000, pp 1117-1122

[4] S. Cierullies, H. Renner, and E. Brinkmeyer, “Numerical optimization of multi-wavelength and cascaded Raman fiber lasers”, Optics Com., vol. 217, 2003, pp 233-235

[5] M. Achtenhagen, T.G. Chang and N. Nyman, “Analysis of a multiple-pump Raman amplifier”, Appl. Phys. Lett., vol. 78, March 2001, pp 1322-1324

[6] F. Castella, P. Chartier and E. Faou, “Analysis of a Poisson system with boundary conditions”, C.R. Acad. Sci. Paris, Ser. I 336, 2003, pp703-708

[7] Francois Castella, Philippe Chartier, Erwan Faou, Dominique Bayart, Florence Leplingard and Catherine Martinelli, ’’Raman Laser: Mathematical and Numerical Analysis of a Model’’, accepted for publication in Mathematical Modelling and Numerical Analysis

[8] D. Hamoir, N. Torabi, A. Bergonzo, S. Borne and D. Bayart, "Raman spectra of line fibres measured over 30 THz", Proc. Symposium On Fibre Measurement, 2000, pp 147-149

[9] J.C. Bouteiller, “Spectral modeling of Raman fiber lasers”, IEEE Photon. Technol. Lett., vol. 15, Dec. 2003, pp 1698-1700